

THE COSMIC HORSESHOE: DISCOVERY OF AN EINSTEIN RING AROUND A GIANT LUMINOUS RED GALAXY

V. BELOKUROV¹, N. W. EVANS¹, A. MOISEEV², L. J. KING¹, P. C. HEWETT¹, M. PETTINI¹, L. WYRZYKOWSKI^{1,4}, R. G. McMAHON¹, G. GILMORE¹, S. F. SANCHEZ³, A. UDALSKI⁴, S. KOPOSOV⁵, D. B. ZUCKER¹, C. J. WALCHER⁶

SUBMITTED TO *the Astrophysical Journal*

ABSTRACT

We report the discovery of an almost complete ($\sim 300^\circ$) Einstein ring of diameter $10''$ in Sloan Digital Sky Survey (SDSS) Data Release 5 (DR5). Spectroscopic data from the 6m telescope of the Special Astrophysical Observatory reveals that the deflecting galaxy has a line-of-sight velocity dispersion in excess of 400 km s^{-1} and a redshift of 0.444, whilst the source is a star-forming galaxy with a redshift of 2.379. From its color and luminosity, we conclude that the lens is an exceptionally massive Luminous Red Galaxy (LRG) with a mass within the Einstein radius of $\sim 5 \times 10^{12} M_\odot$. This remarkable system provides a laboratory for probing the dark matter distribution in LRGs at distances out to 3 effective radii, and studying the properties of high redshift star-forming galaxies.

Subject headings: gravitational lensing – galaxies: structure – galaxies: evolution

1. INTRODUCTION

There have been many optical giant arcs discovered, caused by the lensing effects of massive galaxy clusters and their central galaxies. But, very few optical rings have ever been found, despite theoretical predictions that they should be abundant (Miralda-Escude & Lehar 1992). Warren et al. (1996) found 0047-2808, which is a high redshift star-forming galaxy lensed by a massive early-type galaxy into a partial ($\sim 170^\circ$) Einstein ring of $2''.70$ diameter. Cabanac et al. (2005) found a nearly complete ($\sim 260^\circ$) Einstein ring of diameter $2''.96$ produced by the lensing of a starburst galaxy by a massive and isolated elliptical galaxy. The Sloan Lens ACS Survey (SLACS, Bolton et al. 2006) has also identified a number of partial optical rings, based on the identification of anomalous emission lines in Sloan Digital Sky Survey (SDSS) spectra together with confirmatory follow-up from the Advanced

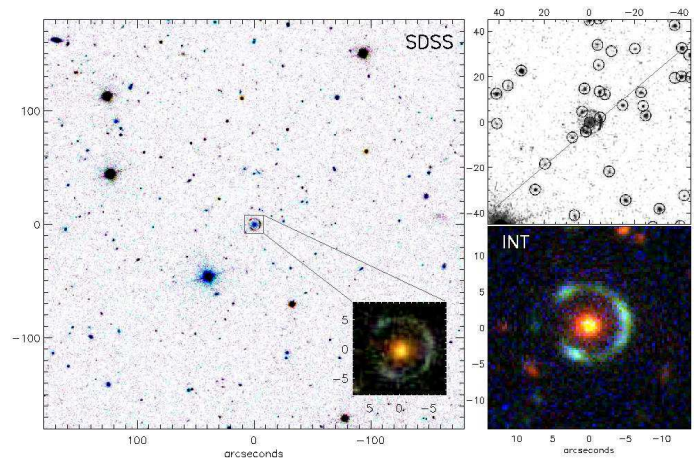


FIG. 1.— Left: SDSS view of the sky composed from g, r, i images around the Cosmic Horseshoe. Most of the objects in the field are faint galaxies. The inset shows $16'' \times 16''$ cut-out centered on the lens. Note the bluish color of the ring. Top right: SDSS g, r, i composite with objects detected by the SDSS pipeline marked with circles. We also show the slit position for SAO follow-up. Bottom right: INT u, g, i composite from follow-up data.

TABLE 1
 PROPERTIES OF THE COSMIC HORSESHOE

Component	Parameter	
Lens	Right ascension	11:48:33.15
	Declination	19:30:03.5
	Redshift, z_L	0.444
	Magnitudes (SDSS), g_L, r_L, i_L	$20^m 8, 19^m 0, 18^m 2$
	Effective radii, $R_{\text{eff},g}, R_{\text{eff},i}$	$2.2'', 1.7''$
	Axis ratio (in g, i)	0.8, 0.9
	Position angle (in g, i)	$99^\circ, 95^\circ$
	Radio Flux (FIRST,NVSS)	5.4 mJy, 4.8 mJy
Source	Redshift, z_S	2.379
	Luminosity	$1.6L^*$
Ring	Diameter	$10''.2$
	Length	300°
	Total magnitudes (INT) u, g, i	$21^m 6, 20^m 1, 19^m 0$
	Mass Enclosed	$5.4 \times 10^{12} M_\odot$

¹ Institute of Astronomy, University of Cambridge, Madingley Road, Cambridge CB3 0HA, UK;vasily, nwe@ast.cam.ac.uk

² Special Astrophysical Observatory, Nizhny Arkhyz, Karachaevo-Cherkessiya, Russia;moisav@sao.ru

³ CAHA de Calar Alto (CSIC-MPIA), E4004 Almera, Spain

⁴ Warsaw University Observatory, Al. Ujazdowskie 4, 00-479, Poland

⁵ MPIA, Königstuhl 17, 69117 Heidelberg, Germany

⁶ Laboratoire d'Astrophysique de Marseille, UMR 6110 CNRS-Université de Provence, BP8, 13376 Marseille Cedex 12, France

Camera for Surveys. All these objects have ring diameters on scales of $< 1''.5$. Here, we report the discovery of a giant Einstein ring, the Cosmic Horseshoe, which has a length of $\sim 300^\circ$ (or $31''$) and a ring diameter of $\sim 10''$. This implies that the lens is an exceptionally massive galaxy – a member of the population of giant Luminous Red Galaxies (LRG).

2. DISCOVERY AND FOLLOW-UP

There have already been many discoveries of new gravitational lens systems using SDSS data. Previous search strategies can be divided into three kinds. The first discovery was made by Inada et al. (2003a), who searched around spectroscopically identified quasars looking for stellar-like objects with a similar color to provide candidates for follow-up. This yielded the spectacular discovery of the $14''.62$ separation lens SDSS J1004+4112. The remaining two search methods target smaller separation lenses, in which the images are unresolved by SDSS. Inada et al. (2003b) and Johnston et al. (2003) searched through spectroscopically identified quasars,

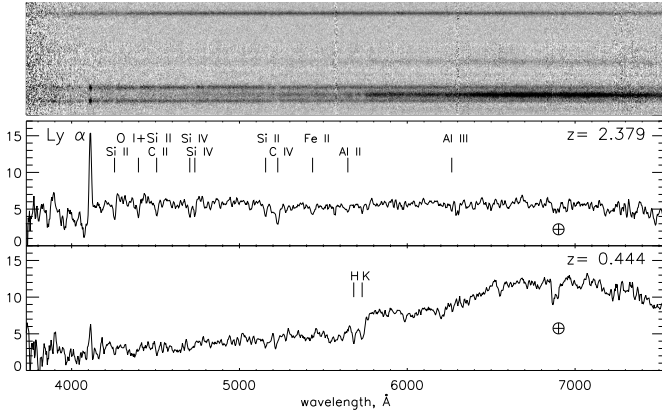


FIG. 2.— Top: Cutout of the SCORPIO 2D spectrum, the horizontal coordinate is the dispersion, the vertical coordinate is the location on the slit. In the lower part, 2 ring images are clearly visible at short wavelength (note the bright Ly α blobs) with the lens appearing at longer wavelengths. Middle: Sum of two extracted 1D image spectra with absorption lines from Table 1 of Shapley et al. (2003). Bottom: 1D lens spectrum with Ca H and K lines marked. The feature at 4100 Å is Ly α leakage caused by 1D extraction. Note the prominent atmospheric absorption at 6900 Å. The spectra are shown in flux units of 10^{-18} erg s $^{-1}$ cm $^{-2}$ Å $^{-1}$.

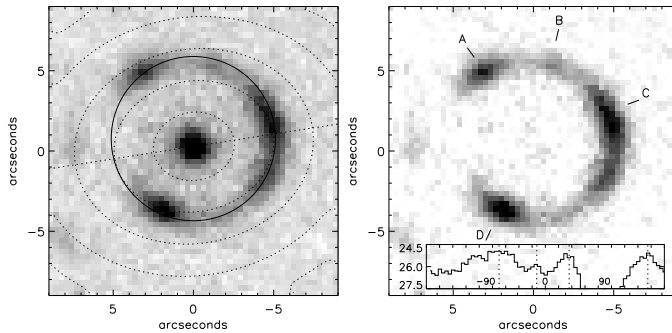


FIG. 3.— Left: g band INT images of a $18'' \times 18''$ field of view centered on the Cosmic Horseshoe. Dotted lines mark the major axis of the LRG and contours show isophotes at 1,2,3,4,5 R_{eff} along the major axis. The best fit circle through the ring is shown as a solid line. Right: Decomposition of the light into the ring after subtraction of the luminosity model for the LRG. Also show is the profile along the ring in the inset. The locations of the four maxima are marked.

looking for evidence of extended sources corresponding to unresolved, multiple images. The most widely-used strategy to date is to search through the spectroscopic database looking for emission lines of high redshift objects within the spectrum of lower redshift early-type galaxies (Johnston et al. 2003; Willis et al. 2005; Bolton et al. 2006).

Here, we introduce a new search method, inspired by the recent, serendipitous discovery of the 8 O'clock Arc, which is a Lyman Break galaxy lensed into three images merging into an extended arc (Allam et al. 2006). The SDSS pipeline resolved the arc into three objects. This suggests an obvious algorithm is to search for multiple, blue, faint companions around luminous red galaxies (LRGs) in the SDSS object catalogue. The search is very fast, so it is easy to experiment with different magnitude and color cuts, as well as search radii. For example, selecting lenses in DR5 to be brighter than $r = 19.5$ and $g - r > 0.6$, together with sources within $6''$ that are fainter than $r = 19.5$ and bluer than $g - r = 0.5$ yields 3 very strong

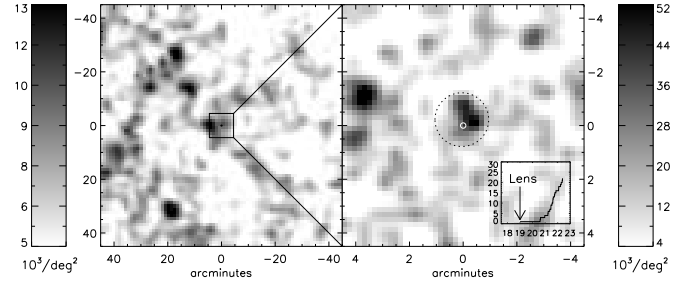


FIG. 4.— Density of galaxies with $r < 22.5$ and $g - r > 1.0$ in the vicinity of the object. Left: large scale structure. Right: Zoom-in on the lens (marked by white ring, shown to scale). The lens belongs to the group of galaxies (marked by dashed circle), 22 members within the 1 arcminute radius. The r -band cumulative LF of the group members is shown in the inset. The lens is the brightest galaxy in the group, most of the other members are fainter than 21 m 5.

candidates. By strong, we mean that there are multiple candidate images around the LRG. One of the three candidates is the 8 O'clock arc. Here, we report on another of the candidates, the Cosmic Horseshoe.

The left panel of Fig. 1 shows a g, r, i composite image of the sky centered on equatorial coordinates $(\alpha, \delta) = (11:48:33.15, 19:30:03.5)$ (J2000). Most of the faint objects in the field of view are galaxies, but the environment is clearly not that of a rich cluster. The inset shows a $16'' \times 16''$ cut-out, in which the central, apparently single, lensing galaxy is surrounded by a $\sim 300^\circ$ ring of radius $\sim 5''$. This makes it the largest, and one of the most complete, optical rings thus far discovered.

We obtained imaging follow-up data at the 2.5m *Isaac Newton Telescope* (INT), La Palma and spectroscopy⁷ at the 6m BTA telescope of the *Special Astrophysical Observatory* (SAO), Nizhnij Arkhyz, Russia. Observations were carried on the INT on the night (UT) of 2007 May 12 with the Wide Field Camera (WFC). The exposure times were 600 s in each of the three wavebands u, g and i – which are similar to the SDSS filters. The measured seeing (FWHM) on the images ($0.33''$ pixels) was $1.30''$, $1.26''$ and $1.21''$ in u, g and i respectively. The data were reduced using the CASU INT WFC pipeline toolkit (Irwin & Lewis 2001). The bottom right panel of Fig. 1 shows the u, g, i composite field of view of $24'' \times 24''$ centered on the lens galaxy.

Long-slit spectral observations were performed on the night of 2007 May 15/16 with the multi-mode focal reducer SCORPIO (Afanasiev & Moiseev 2005) installed at the prime focus of the BTA 6-m telescope at the SAO⁸. The seeing was $\sim 1''.7$. A $1''.0$ wide slit was precisely placed to intercept the two brighter arcs in the ring (C and D in Fig. 3) and to include some of the light from the lensing galaxy, as shown in the top right panel of Fig. 1. We used the VPHG550G grism which covers the wavelength interval 3650–7550 Å with a spectral resolution 8–10 Å FWHM. With a CCD EEV 42–40 $2k \times 2k$ detector, the reciprocal dispersion was ~ 1.9 Å per pixel. The total exposure time was 3600 s, divided into six 10-minute exposures. The target was moved along the slit between expo-

⁷ Auxiliary CAHA/PMAS data taken on 11 May 2007 strongly suggested that the source was at a redshift ~ 2 , which was taken into account for the preparation of the 6m telescope run.

⁸ A description of the SCORPIO instrument can be found at <http://www.sao.ru/hq/moisav/scorpio/scorpio.html>

ures to facilitate background subtraction and CCD fringes removal in the subsequent data processing. The data reduction, which includes the standard steps of bias subtraction, geometrical corrections, flat fielding, sky subtraction, and calibration to flux units (F_λ) was performed by means of IDL-based software briefly described in Afanasiev & Moiseev (2005).

The top panel of Fig. 2 shows a cut-out of the two-dimensional spectrum with position along the slit plotted against the dispersion. The slit also passes through a nearby star, which causes the spectrum in the topmost pixels. In the lower part, the blue spectrum is dominated by two images of the source, whilst the red spectrum is dominated by the lensing galaxy. The lower panels show extracted one-dimensional spectra. The middle one is the sum of the two source images – there is a strong narrow line which is Ly α emission, together with accompanying Ly α forest bluewards and multiple absorption lines redwards. This yields an unambiguous measurement of the source redshift as $z = 2.379$. The lower panel is the lens galaxy spectrum, which shows the characteristic features of a LRG. The redshift of the lens is $z = 0.444$. Although Ca H and K absorption is clearly detected in the lensing galaxy spectrum, the signal-to-noise ratio is modest, ~ 10 , and the resolution relatively low. However, there is definite evidence that the Ca H and K lines are resolved. Performing fits of Gaussian line profiles to the absorption produces an estimate for the galaxy velocity dispersion of $430 \pm 50 \text{ km s}^{-1}$, where the principal uncertainty arises from the placement of the ‘continuum’. The spectrograph slit was not aligned across the centre of the galaxy but, given the relatively poor seeing, the spectrum is dominated by light from within the half-light radius of the galaxy. A higher signal-to-noise ratio spectrum is required to provide an accurate estimate of the galaxy velocity dispersion.

The Cosmic Horseshoe is shown with great clarity in the panels of Fig 3. From these, we can extract the properties of the LRG, such as magnitude, effective radius, ellipticity and orientation, by fitting a PSF-convolved de Vaucouleurs profile as listed in Table 1. Our INT magnitudes agree with the SDSS magnitudes reported in the Table, although SDSS overestimates the g band effective radius because of contamination from the ring. The shape of the isophotes of the LRG is shown in dotted lines. In the right panel, the light from the lensing galaxy is subtracted to leave a clearer picture of the ring in the g band. The surface brightness profile along the ring in magnitudes arcsec^{-2} is shown in the inset. There are four maxima, A, B, C and D, whose right ascension and declination offsets from the LRG are: A : ($3''.0, 4''.6$), B : ($-1''.1, 5''.2$), C : ($-4''.7, 2''.2$ and D : ($2''.0, -4''.0$) together with typical errors of $\lesssim 0''.4$.

Fig 4 shows the number density of objects with $r < 22.5$ and $g - r > 1$ classified by SDSS as galaxies around the Cosmic Horseshoe. In the left panel, a large-scale filamentary structure can be discerned. The right panel shows that the Cosmic Horseshoe lies in a group of galaxies – the enhancement of the number density of the background is ~ 6 . The lens is the brightest object in the group of ~ 20 members, as shown in the cumulative luminosity function of the objects within the dashed circle of $1'$ radius.

3. DISCUSSION

3.1. Source

The spectrum of the Cosmic Horseshoe reproduced in the middle panel of Fig. 2 shows it to be a star-forming galaxy

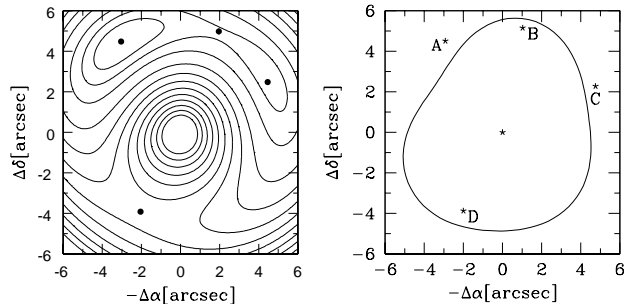


FIG. 5.— Left: Contours of the Fermat time delay for the lens model of Cosmic Horseshoe, together with the locations of the stationary points which mark the predicted image positions. Right: The critical curve of the lens model, which is also a contour of constant convergence. The measured locations of the ring maxima A, B, C, and D are marked. The model predictions are in excellent agreement with the image locations, with the sole exception of the right ascension of image B, which is discrepant by $0''.8$.

at $z = 2.379$. From the observed wavelengths of ten absorption lines, labelled in Figure 3, we deduce a mean redshift $\langle z_{\text{abs}} \rangle = 2.3767 \pm 0.0006$, while the peak of the Ly α emission line gives $z_{\text{em}} \approx 2.3824$. The overall character of the spectrum is that of a typical BX galaxy from the surveys by Steidel et al. (2004) – these are galaxies at a mean redshift $\langle z \rangle \approx 2.2$ selected from their blue rest-frame UV colours. In finer detail, the spectrum resembles most closely the subset of these galaxies which are relatively young, with assembled stellar masses $\langle M^* \rangle \approx 5 \times 10^9 M_\odot$ and metallicities of about 1/3 solar. The composite spectrum of galaxies with these characteristics has been discussed by Erb et al. (2006a) and, like that of the Cosmic Horseshoe, has typical rest-frame equivalent widths of the interstellar lines $W_{\text{IS}} \approx 1.5 - 2 \text{ \AA}$, and a similar strength of the Ly α emission line. The closest local analogue is the field spectrum of nearby starburst galaxies discussed by Chandar et al. (2005). The difference between Ly α emission and interstellar absorption redshifts found here is also typical of high redshift star-forming galaxies (e.g., Steidel et al. 2004) and is generally interpreted as resulting from large-scale outflows of the interstellar medium in galaxies with high rates of star formation, driven by kinetic energy deposited by massive star winds and supernovae. Adopting the median blueshift of 165 km s^{-1} of the interstellar absorption lines relative to the H II regions producing H α emission (Steidel et al. 2007, in preparation), we deduce a systemic redshift of $z_{\text{sys}} = 2.379$.

The galaxy appears to be of approximately fiducial luminosity. Interpolating between the measured g and i magnitudes in Table 1, we deduce an absolute magnitude at 1700 \AA $AB_{1700} = -25.4$ in the standard cosmology ($\Omega_m = 0.3$, $\Omega_\Lambda = 0.7$, $H_0 = 70 \text{ km s}^{-1} \text{ Mpc}^{-1}$). If the magnification factor is ~ 35 , or 3.9 mag, this corresponds to an intrinsic $AB_{1700} = -21.5$, or $L \approx 1.6 L^*$, according to the recent determination of the luminosity function of BX galaxies by Reddy et al. (2007). On the other hand, the colours of the lensed galaxy are redder than those of most BX galaxies. The $u - g$ and $g - i$ colours indicated by the photometry in Table 1 imply a UV spectral slope significantly redder than the essentially flat spectrum ($F_\nu \propto \nu^0$) expected for an unobscured star-forming galaxy (e.g. Leitherer et al. 1999). Assuming that the Calzetti et al. (2000) obscuration law applies, we deduce $E(B - V) = 0.45$, at the upper end of the distribution of values reported by Erb et al. (2006b) for BX galaxies. The

corresponding attenuation at 1700 \AA is a factor of ~ 10 . Alternatively, the galaxy may be intrinsically redder than a young starburst, if we are observing it coincidentally after a recent episode of star formation. In either case, the unusually red colour of its spectrum may suggest that such objects are not well represented in UV-selected surveys, a possibility that can only be assessed quantitatively once a larger sample of lensed high- z galaxies becomes available.

3.2. Lenses

Bernardi et al. (2006) looked through the spectroscopic part of the SDSS DR1 and found 70 galaxies with dispersions $> 350 \text{ km s}^{-1}$ that were not obvious superpositions. They concluded that these are the galaxies with largest velocity dispersions and might harbour the most massive black holes. The fact that the PSF-convolved de Vaucouleurs model gives an excellent fit to the light distribution of the lens galaxy minimises the chance that the high velocity dispersion is a product of superposition in our case. The lens is detected in the NVSS and FIRST surveys with an integrated flux density at 20cm of 4.8 and 5.4mJy respectively. Assuming a radio spectrum of the form $S_\nu \propto \nu^\alpha$ ($\alpha = -0.7$) the monochromatic radio power is $3.2 \times 10^{24} \text{ W Hz}^{-1}$ similar to the radio galaxies studied at $z \sim 0.7$ in the 2SLAQ luminous red galaxy survey (Sadler et al. 2006). In the nearby Universe such powerful radio sources are associated with active galactic nuclei rather than star-forming galaxies and this supports the picture that the lensing galaxy hosts a massive black hole.

The absolute magnitude of the Cosmic Horseshoe in r -band is -23.45 at $z = 0$. This assumes the SDSS r -band model magnitude of $r=19.00$, together with the standard cosmology, a k correction of $-0^m.87$, and the passive evolution model of $+0^m.38$ (Bernardi et al. 2003). This puts the lens in the brightest bin for LRGs. The high luminosity is also indicated by the red color ($g - i > 2.6$) of the galaxy. Color and luminosity also correlate with velocity dispersion and mass (Figures 4 and Figure 7 of Bernardi et al 2003). All these measurements support the idea that the lensing galaxy is a very massive object. In fact, Bernardi et al. (2006) suggested that the brightest and most massive LRGs may act as efficient gravitational lenses. The discovery of the Cosmic Horseshoe is a spectacular confirmation of their suggestion.

3.3. Model

Let us model the lens in the first instance as a singular isothermal sphere galaxy with a velocity dispersion $\sigma_v = 430 \text{ km s}^{-1}$. For a lens redshift of 0.44 and a source redshift of 2.38, the deflection due to an isolated isothermal sphere is $\sim 3.7''$. As the LRG is so massive, it provides most of the deflection needed. In physical units, the ring radius is at a

projected distance of $\sim 30 \text{ kpc}$ from the center of the LRG. The (cylindrical) mass enclosed within the Einstein ring is $\sim 5.4 \times 10^{12} M_\odot$. The magnification can be crudely estimated under the assumption that the source size at this redshift is $\sim 0''.4$ (Law et al. 2007). The ratio of the area subtended by the ring to that subtended by the source is $\sim 4R/\delta r$, where R is the ring radius and δr is the source size which is roughly same as the ring thickness. This gives a magnification of ~ 50 .

The ring has at least four density knots or maxima, A, B, C and D, whose locations are noted in Section 2. A more sophisticated model that fits the image locations and relative brightnesses is provided by the method of Evans & Witt (2003). Here, the lens density has an isothermal profile in radius, but the angular shape of the isodensity contours is given by eqn. (5) of Evans & Witt (2003) with the Fourier coefficients ($a_0 = 9.89$, $a_2 = 0.090$, $b_2 = -0.11$, $a_3 = 0.02$, $b_3 = -0.04$). The Fermat surface and the critical curve of the model are given in Figure 5. The brightest and most extended knot is C, which may even be a conglomeration of three merging images. In the modelling, it has been treated as a single image. The positive parity images are A and C, whilst the negative parity images corresponding to saddle-points on the Fermat surface and are B and D. The mass enclosed within the critical curve is $\sim 6 \times 10^{12} M_\odot$, similar to our crude estimates. The magnification of this model is ~ 35 .

The combination of high absolute luminosity and large magnification factor makes the Cosmic Horseshoe the brightest galaxy known at $z > 2$. The lens galaxy is one of the most massive LRGs ever detected. Detailed studies of this remarkable system at a variety of wavelengths, from optical to sub-mm will help us probe the physical nature of star formation in the young universe, whilst detailed modeling will enable us to study the density profile and the interplay between baryons and dark matter in very massive galaxies.

The authors acknowledge with gratitude the support of the EC 6th Framework Marie Curie RTN Programme MRTN-CT-2004-505183 ("ANGLES"). The paper was partly based on observations collected with the 6m telescope of the Special Astrophysical Observatory (SAO) of the Russian Academy of Sciences (RAS) which is operated under the financial support of Science Department of Russia (registration number 01-43). Funding for the SDSS and SDSS-II has been provided by the Alfred P. Sloan Foundation, the Participating Institutions, the National Science Foundation, the U.S. Department of Energy, the National Aeronautics and Space Administration, the Japanese Monbukagakusho, the Max Planck Society, and the Higher Education Funding Council for England. The SDSS Web Site is <http://www.sdss.org/>.

REFERENCES

- Afanasiev V. L., Moiseev A. V., 2005, *AstL*, 31, 194 (astro-ph/0502095)
 Allam, S. S., Tucker, D. L., Lin, H., Diehl, H. T., Annis, J., Buckley-Geer, E. J., & Frieman, J. A. 2007, *ApJ*, in press, astro-ph/0611138
 Bernardi, M., et al. 2003, *AJ*, 125, 1849
 Bernardi, M., et al. 2006, *AJ*, 131, 2018
 Bolton, A. S., Burles, S., Koopmans, L. V. E., Treu, T., & Moustakas, L. A. 2006, *ApJ*, 638, 703
 Cabanac, R. A., Valls-Gabaud, D., Jaunsen, A. O., Lidman, C., & Jerjen, H. 2005, *A&A*, 436, L21
 Calzetti, D., Armus, L., Bohlin, R. C., Kinney, A. L., Koorneef, J., & Storchi-Bergmann, T. 2000, *ApJ*, 533, 682
 Chandar, R., Leitherer, C., Tremonti, C. A., Calzetti, D., Aloisi, A., Meurer, G. R., & de Mello, D. 2005, *ApJ*, 628, 210
 Erb, D. K., Shapley, A. E., Pettini, M., Steidel, C. C., Reddy, N. A., & Adelberger, K. L. 2006a, *ApJ*, 644, 813.
 Erb, D. K., Steidel, C. C., Shapley, A. E., Pettini, M., Reddy, N. A., & Adelberger, K. L. 2006b, *ApJ*, 646, 107.
 Evans, N. W., & Witt, H. J. 2003, *MNRAS*, 345, 1351
 Inada, N., et al. 2003, *Nature*, 426, 810
 Inada, N., et al. 2003, *AJ*, 126, 666
 Irwin, M.J., Lewis, J.R., 2001, *New Ast Rev*, 45, 105
 Johnston, D. E., et al. 2003, *AJ*, 126, 2281
 Law, D. R., Steidel, C. C., Erb, D. K., Pettini, M., Reddy, N. A., Shapley, A. E., Adelberger, K. L., & Simenc, D. J. 2007, *ApJ*, 656, 1
 Leitherer, C. et al. 1999, *ApJS*, 123, 3
 Miralda-Escude, J., & Lehar, J. 1992, *MNRAS*, 259, 31P
 Morgan, N. D., Snyder, J. A., & Reens, L. H. 2003, *AJ*, 126, 2145
 Oguri, M. 2006, *MNRAS*, 367, 1241
 Reddy, N. A., Steidel, C. C., Pettini, M., Adelberger, K. L., Shapley, A. E., Erb, D. K., & Dickinson, M. 2007, *ApJ*, in press.

Sadler, E. et al. 2006, MNRAS, in press (astro-ph/0612019)
Shapley A. E., Steidel C. C., Pettini M., Adelberger K. L., 2003, ApJ, 588,
65
Steidel, C. C., Shapley, A. E., Pettini, M., Adelberger, K. L., Erb, D. K.,
Reddy, N. A., & Hunt, M. P. 2004, ApJ, 604, 534

Warren, S. J., Hewett, P. C., Lewis, G. F., Moller, P., Iovino, A., & Shaver,
P. A. 1996, MNRAS, 278, 139
Willis, J. P., Hewett, P. C., & Warren, S. J. 2005, MNRAS, 363, 1369